Index-based methods for water body extraction in satellite data

M. Arreola-Esquivel, M. Delgadillo-Herrera, C. Toxqui-Quitl, A. Padilla-Vivanco

M. Arreola-Esquivel, M. Delgadillo-Herrera, C. Toxqui-Quitl, A. Padilla-Vivanco, "Index-based methods for water body extraction in satellite data," Proc. SPIE 11137, Applications of Digital Image Processing XLII, 111372N (6 September 2019); doi: 10.1117/12.2529756

SPIE.

Event: SPIE Optical Engineering + Applications, 2019, San Diego, California, United States

Index-based methods for water body extraction in satellite data

M. Arreola-Esquivel, M. Delgadillo-Herrera, C. Toxqui-Quitl, and A. Padilla-Vivanco

Computer Vision Laboratory, Universidad Politécnica de Tulancingo, Hgo. 43629, México.

ABSTRACT

Several water index-based methods have been proposed in the literature, which, combine satellite multispectral bands in an algebraic expression. The objective of these water index-based methods is to increase the intensity contrast between water-pixels (surface water-body) and non-water pixels (built-up, soil, vegetation, etc.). The present investigation evaluates the Modified Normalized Difference Water Index (MNDWI) and the Automated Water Extraction Index (AWEI) using the Satellite data from Landsat 5 TM, Landsat 8 and Sentinel 2A at different time scenes. Based on visual inspection of the Lake Metztitlan water body mapping results, a high performance of AWEI approached via the OLI and the MSI sensors is observed. In the selected study area of $[9210x9380]m$, a statistical water pixel percentage of 30.703616% is observed in a flooding season and 9.884537% for a dry season of the year.

Keywords: Water index-based methods, Landsat data, Sentinel imagery.

1. INTRODUCTION

Water body change detection is an excellent indicator of environmental alteration [1, 2]. The shortage of natural resources due to climate change, urban grow, deforestation, among others has great impact on society. These environmental changes can be evaluated by spectral information registered with a satellite sensor[3]. The long-term Landsat and Sentinel satellite imagery has proved to be an invaluable data resource for environmental water change and ecological analysis. Landsat missions has been operated by the US Geological Survey (USGS) since 1990 [4] and Sentinel 2A was launched by ESA on 2015 [5]. Since, Landsat and Sentinel data became a free download through Internet portals (i.e. Earth Explorer, USGS), it has become an object of study in remote sensing of the Earth surface. The USGS registers 50-fold annually increase in downloads of satellite images [6]. The spatial and spectral resolution in satellite imagery may differ according to the satellite sensor. A comparison of the wavelength bands and spatial resolution among sensors are shown in Table 1.

Table 1. Band specifications of TM, OLI and MSI satellite sensors [7].

BANDS	Landsat 5 TM		Landsat 8 OLI		Sentinel-2 MSI	
	Wavelength (μm)	Spatial resolution (m)	Wavelength (μm)	Spatial resolution (m)	Wavelength (μm)	Spatial resolution (m)
Blue	0.45 - 0.52	30	0.45-0.51	30	0.46-0.52	10
Green	0.52 - 0.60	30	0.53-0.59	30	0.55-0.58	10
Red	0.63 - 0.69	30	0.64-0.67	30	0.64-0.67	10
NIR	0.76 - 0.90	30	0.85-0.88	30	0.78-0.90	10
SWIR-1	1.55 - 1.75	30	1.57-1.65	30	1.57-1.65	20
SWIR-2	2.08 - 2.35	30	2.11-2.29	30	2.10-2.28	20

Based on algebraic expression and bands combination [8, 9], several methods have been developed for surface water extraction [10]. Among the highly threshold-number methods proposed in the literature are the Modified Normalized Difference Water Index (MNDWI) [11], and the Automated Water Extraction Index $AWEI_{nsh}$ no shadows [12].

Applications of Digital Image Processing XLII, edited by Andrew G. Tescher, Touradj Ebrahimi, Proc. of SPIE
Vol. 11137, 111372N · © 2019 SPIE · CCC code: 0277-786X/19/$21 · doi: 10.1117/12.2529756

In order to obtain a high MNDWI and AWEI surface water classification accuracy, an optimum threshold-number must be found. However, selecting a smaller interval number to find the optimum threshold value can be time-consuming due to different environmental scene (e.g. geographical area, date and time acquisition) conditions [13]. The histogram from a multispectral image can be used to identify the optimum histogram-threshold value in a single or multiple scenes with a high geographical diversity.

The purpose of this discussion paper is to provide a concise overview of the AWEI and the MNDWI performance, when combining multispectral bands registered by TM, OLI and MSI satellite sensors at different time scenes. The workflow of this document is as follows: In Section 2, the index-based methods definition for water extraction are given. In Section 3, is illustrated the Region Of Interest (ROI) of the study area and the optimum histogram-threshold value of the selected scene. Section 4, outlines MNDWI and AWEI examples of water body extractions using Landsat 5 TM, Landsat 8 OLI and Sentinel 2A imagery. Section 5, a statistical water pixel percentage change detection is analyzed using the AWEI method. Finally in Section 6, a main conclusion is discussed.

2. INDEX-BASED METHODS FOR WATER BODY EXTRACTION

Multi-band index-based methods lies in calculation of the normalized difference between the maximum and minimum reflectance values among multispectral imagery.

2.1 Modified Normalized Difference Water Index (MNDWI)

The aim of the Modified Normalized Difference Water Index (MNDWI) lies in increase the intensity contrast between the open water bodies and the background (non-water pixels). The MNDWI is express as [11],

$$MNDWI = \frac{(Green - (SWIR - 1))}{(Green + (SWIR - 1))}, \tag{1}$$

where $Green$ and $SWIR - 1$ are the spectral bands defined in table 1. As a result, the water-pixels will have greater positive values, due to it absorbs the SWIR. On the other hand, built-up, soil and vegetation land cover will have negative values as these ones reflect SWIR.

2.2 Automated Water Extraction Index $AWEI_{nsh}$ no shadows

In the development of the Automated Water Extraction Index ($AWEI_{nsh}$), five spectral bands and different coefficients are used. The $AWEI_{nsh}$ aim is to separate water-pixels with positive values from negative pixels that represent non-water (e.g. built-up surfaces). $AWEI_{nsh}$ is defined as [12],

$$AWEI_{nsh} = 4(R_{Green} - R_{SWIR-1}) - (0.25R_{NIR} + 2.75R_{SWIR-2}), \tag{2}$$

where R is the reflectance value of the $Green$, NIR, $SWIR - 1$ and $SWIR - 2$ spectral bands defined in table 1.

3. DATA ANALISYS

The ROI of this study is Lake Metztitlan located at: Lat: $20.68226346° N$ and Lon: $-98.85789350° W$ in Hidalgo state of México, which can be seen in Figure 1. The acquisition data registered by Landsat 5 TM (January 23, 2011), Landsat 8 OLI (April 18, 2013) and Sentinel 2A (March 11, 2017) are shown in Figure 1 (a), (b) and (c). The same georeferenced area of the Level 1 (L1T) Landsat and Level 1C (L1C) Sentinel 2 Terrain-Corrected was selected in ENVI version 5.1 (Exelis Visual Information Solutions, Boulder, Colorado).

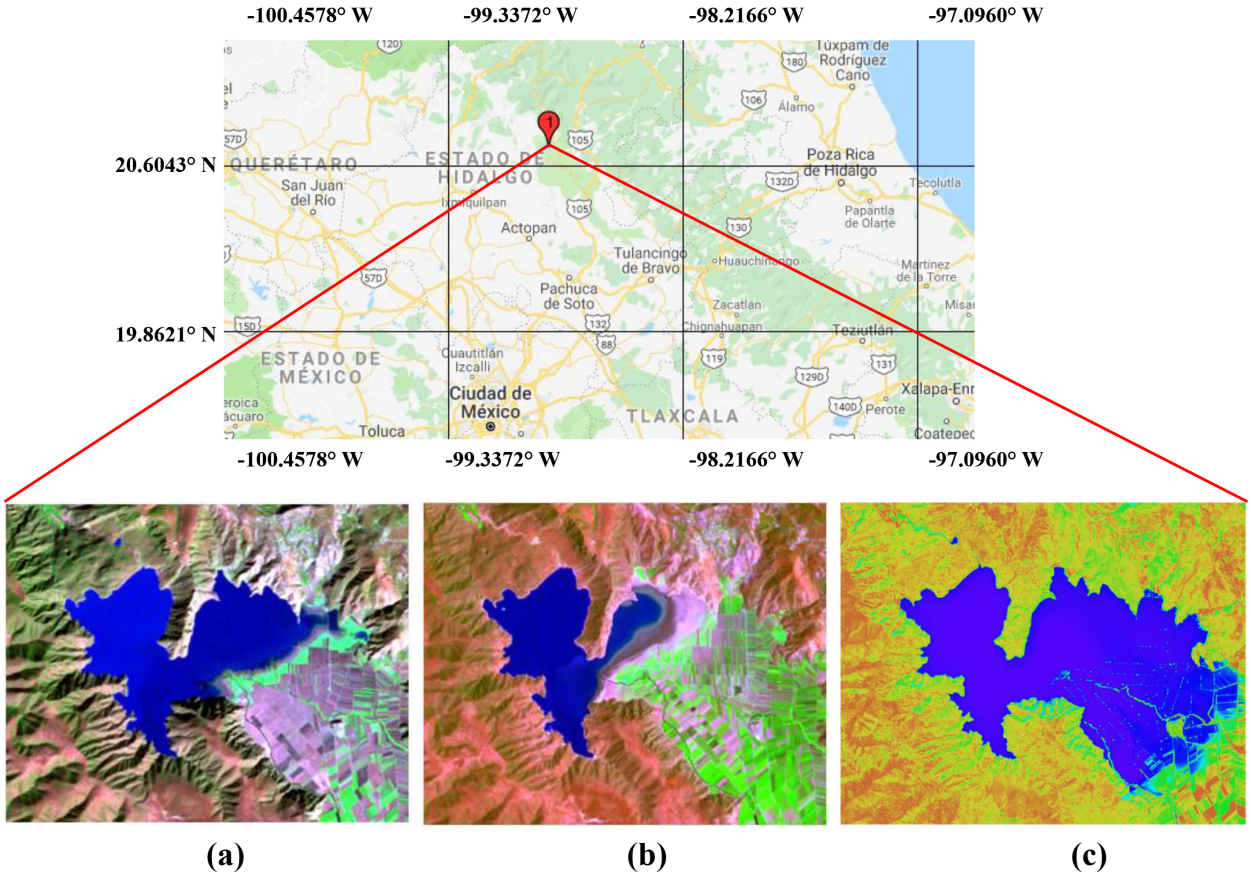

Figure 1. Geographical RGB scene location of Lake Metztitlan from [14]: Resolution of 307x246 pixels for (a) Landsat 5 TM and (b) Landsat 8 OLI, and 663x531 pixels for (c) Sentinel 2A.

The USGS satellite data used for certain water-land analyses, must be preprocessed to obtain high quality results in different time-sensor scenes [15]. Before computing the MNDWI and $AWEI_{nsh}$ water extractions, the Landsat multispectral data was solar and atmospheric corrected using ENVI. The Sentinel 2A imagery were Bottom Of Atmosphere (BOA) corrected with the Sen2Cor algorithm on SNAP - ESA Sentinel Application Platform v2.0.2. In addition, Sentinel 2A visible and near infrared bands were resampled to 20 m by means of the nearest neighborhood approach in SNAP to make Sentinel and Landsat data resolution consistent.

4. WATER EXTRACTION RESULTS

In this study, we analyzed the variation of a high geographical diversity scene threshold (HGDST) obtained by Acharya [3] . Where is propose an optimal threshold number (OTN) using the MNDWI method ($OTN_{MNDWI} = 0.35$) and AWEI approach ($OTN_{AWEI_{nsh}} = 0.1897$). Furthermore, we compute the histogram-threshold (HTV) derived from each scene. In order to select the optimum HTV, the intensity contrast between water-pixels (with positive values) and non-water pixels (with negative values) was taken into account. The positive number between the two height peaks in a histogram was chosen as the optimum threshold value with high stability among NDWI and $AWEI_{nsh}$ images. An example of the histogram to find the optimum HTV is shown in Figure 2.

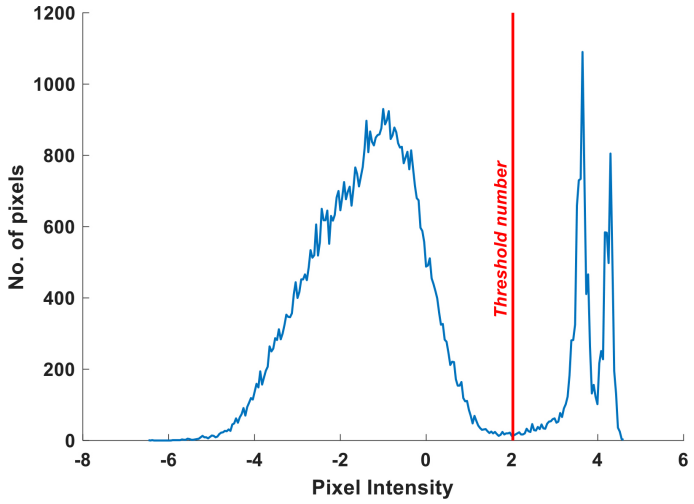

Figure 2. Histogram representing an AWEI image result with positive pixel intensity (water body) and negative pixel intensity (background), using Landsat 5 TM imagery. The selected $HTV_{AWEI_{nsh}} = 2.02159$.

4.1 Water body extraction of Lake Metztitlan using Landsat 5 TM imagery

The MNDWI and $AWEI_{nsh}$ index-based methods for water body extraction were apply to the satellite data of Figure 1a. Comparing the results in Figure 3 a lower performance is presented in (a) the non-binarized $MNDWI$ algorithm, which does not suppress artifacts (e.g. urban and shadow areas).

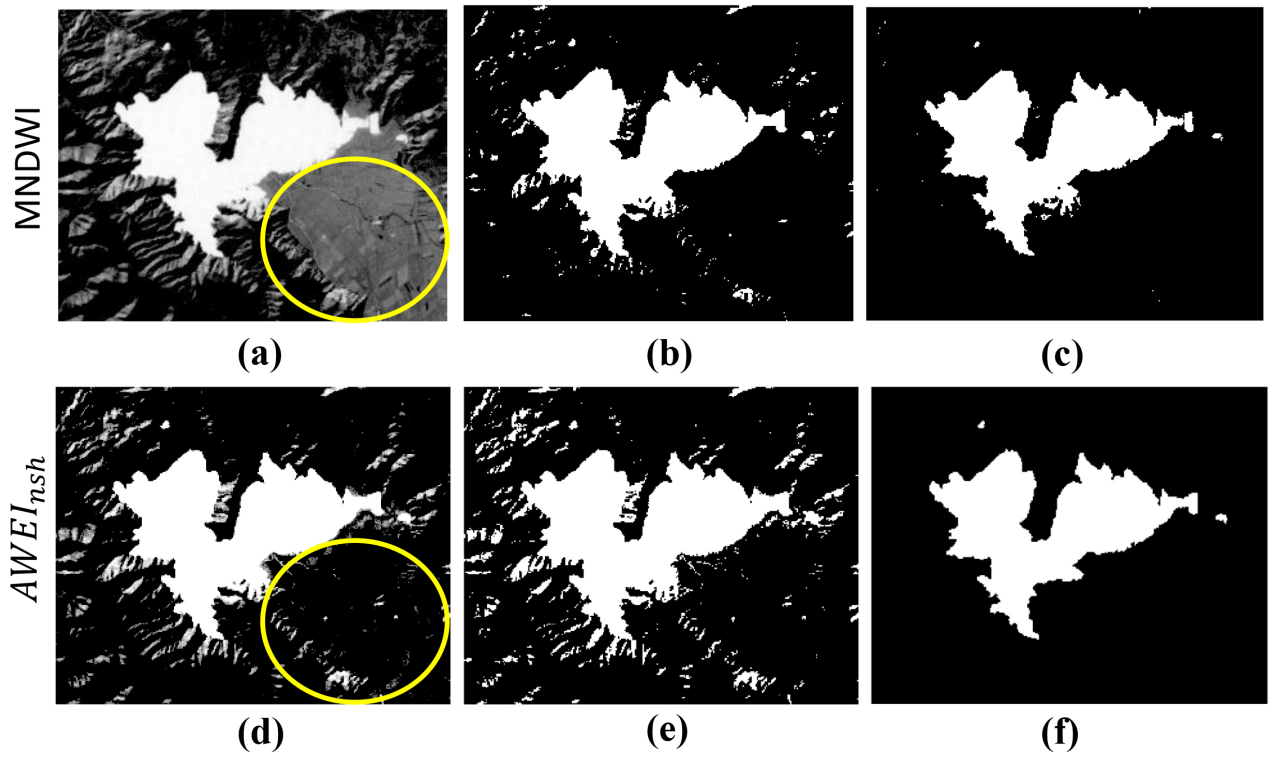

Figure 3. Lake Metztitlan: (a) Non-binarized MNDWI, (b) OTN_{MNDWI}, (c) $HTV_{MNDWI} = 0.63888$, (d) Non-binarized $AWEI_{nsh}$, (e) $OTN_{AWEI_{nsh}}$, and (f) $HTV_{AWEI_{nsh}} = 2.02159$.

Furthermore, the (d) non-binarized $AWEI_{nsh}$ could not be able to discriminate mountain shadows and vegetation. On the other hand, (b) and (e), OTN_{MNDWI} shows a greater accuracy regarding $OTN_{AWEI_{nsh}}$. In Figures 3 (c) and (f) is shown that HTV_{MNDWI} is extracting shadows and water mix information that $HTV_{AWEI_{nsh}}$ does not. Comparing OTN and HTV, the last present fairly stability to suppress non-water surfaces.

4.2 Water body extraction of Lake Metztitlan using Lansat 8 OLI imagery

The MNDWI and $AWEI_{nsh}$ index-based methods for water body extraction were apply to the satellite data of Figure 1b. Similar as in section 4.1, the worst result is shown by (a) non-binarized MNDWI. Meanwhile, the histogram procedure in Figure 4 (c) and (f) using multispectral OLI imagery, presents a high surface water mapping accuracy.

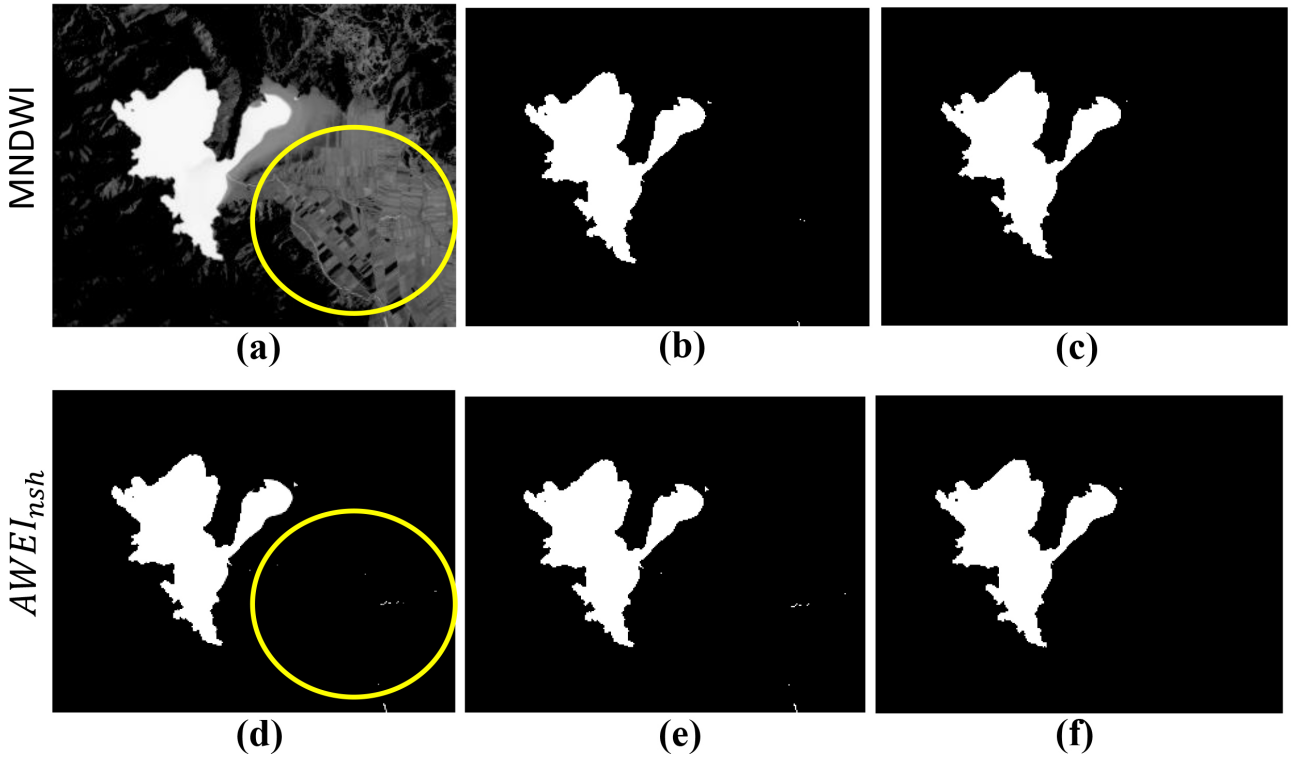

Figure 4. Lake Metztitlan: (a) Non-binarized MNDWI, (b) OTN_{MNDWI}, (c) $HTV_{MNDWI} = 0.58570$, (d) Non-binarized $AWEI_{nsh}$, (e) $OTN_{AWEI_{nsh}}$, and (f) $HTV_{AWEI_{nsh}} = 2.37209$.

4.3 Water body extraction of Lake Metztitlan using Sentinel 2A imagery

The MNDWI and $AWEI_{nsh}$ index-based methods for water body extraction were apply to the satellite data of Figure 1c. The non-binarized (a) and (d) images in Figure 5, show the worst results as in section 4.1 and 4.2. On the other hand, the results of the histogram procedure with the MSI sensor exhibit a precise water body separation (positive water pixel values) from the background (negative pixel values).

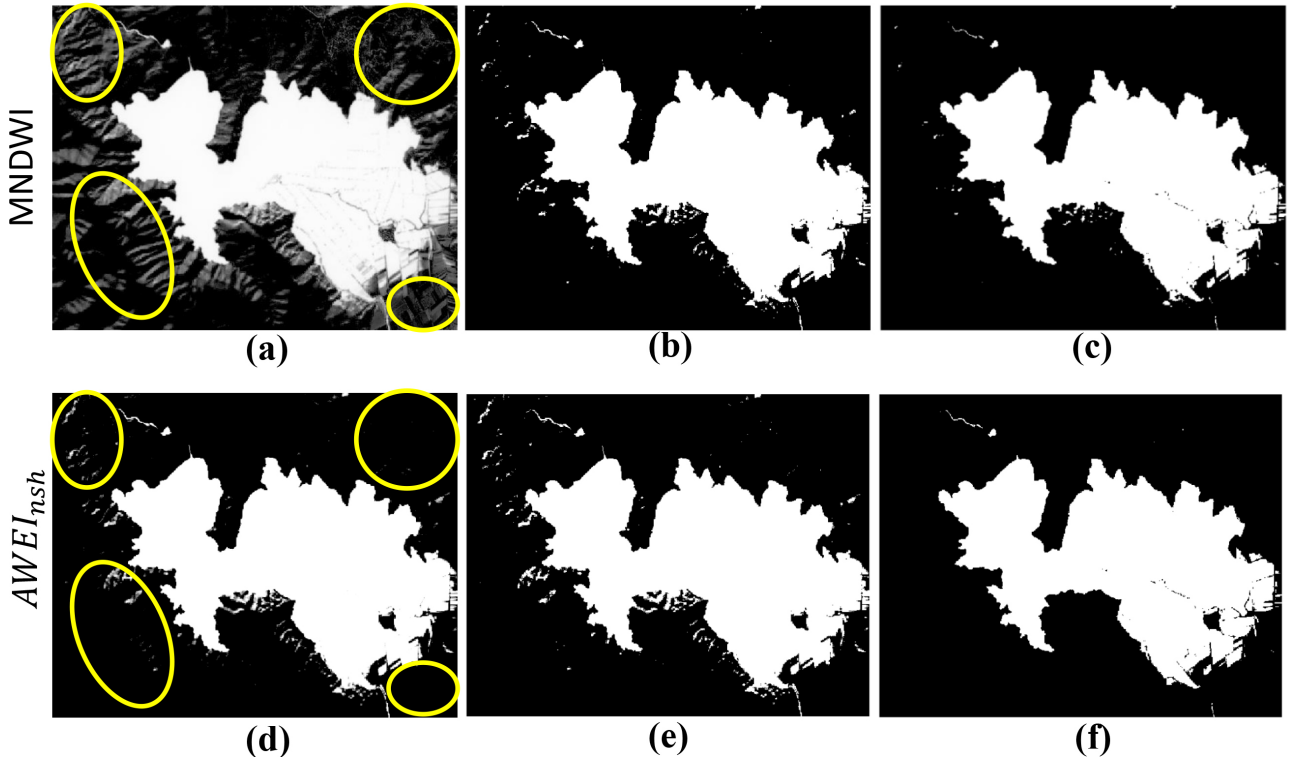

Figure 5. Lake Metztitlan: (a) Non-binarized MNDWI, (b) OTN_{MNDWI}, (c) $HTV_{MNDWI} = 0.50610$, (d) Non-binarized $AWEI_{nsh}$, (e) $OTN_{AWEI_{nsh}}$, and (f) $HTV_{AWEI_{nsh}} = 1.75806$.

5. SURFACE WATER MONITORING OF LAKE METZTITLAN

In this Section, a comparison of the $HTV_{AWEI_{nsh}}$ results among sensor is done. In a high quality data results, the amount of water (pure water pixels) can be compared over time. In Figure 6 (b) the image registered on April 18, 2013 shows the least amount of water, while in (a) January 23, 2011 the water increases. In (c) image registered in March 11, 2017 can be observed flooded urban areas.

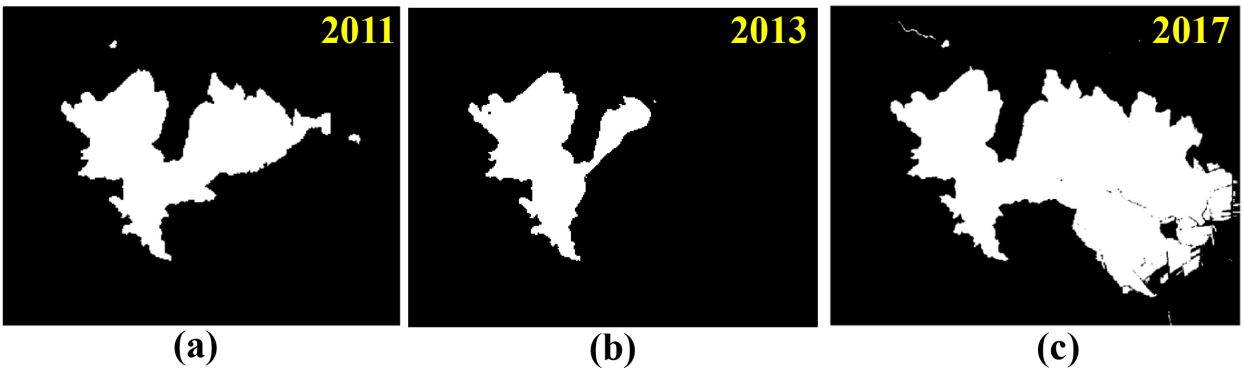

Figure 6. Lake Metztitlan: (a) Landsat 5 TM, (b) Landsat 8 OLI, (c) Sentinel 2A.

Table 2. Water pixel percentages from Figure 6 a-c.

2011	2013	2017
16.280024%	9.884537%	30.703616%

6. CONCLUSIONS

Among $AWEI_{nsh}$ and MNDWI results shown in Figures 3 , 4, and 5, a better performance is obtained with $AWEI_{nsh}$ algorithm. $AWEI_{nsh}$ exhibit a high stability among non-binarized and optimal threshold imagery of Lake Metztitlan water body mapping. In order to remove artifacts (non-water pixels) in the scene using $AWEI_{nsh}$ method, an optimum threshold value is used, but some information (water pixels) could be remove from the scene. In the Figure 6 (a), (b) and (c), is observed a closer approach to the Lake Metztitlan analysis at different time scenes among sensors in $AWEI_{nsh}$ imagery. The monitoring of the change detection in Lake Metztitlan shows a statistical percentage pixel of 30.703616% for flooding season and 9.884537% for dry season. Beyond this certain study, the radiometric characteristics and the atmospheric correction difference among sensors can affect the water mapping results. Those differences must be taken into account in upcoming analysis.

ACKNOWLEDGMENTS

M. Arreola-Esquivel and M. Delgadillo-Herrera thank to Consejo Nacional de Ciencia y Tecnología (CONACyT); with CVU no. 858585 and 858588. We thank the support of PADES program; Award no. 2018-13-011-047. And we thank to Politecnico di Torino by the support during the research stay in October-November 2018 and May-June 2019.

REFERENCES

[1] Pekel, J.-F., Cottam, A., Gorelick, N., and Belward, A. S., "High-resolution mapping of global surface water and its long-term changes," *Nature* **540**(7633), 418 (2016).

[2] Valdiviezo-N, J. C., Castro, R., Cristóbal, G., and Carbone, A., "Hurst exponent for fractal characterization of landsat images," in [*Remote sensing and modeling of ecosystems for sustainability Xi*], **9221**, 922103, International Society for Optics and Photonics (2014).

[3] Acharya, T., Subedi, A., and Lee, D., "Evaluation of water indices for surface water extraction in a landsat 8 scene of nepal," *Sensors* **18**(8), 2580 (2018).

[4] USGS, "What are the band designations for the Landsat satellites?." USGS, 2018 https://www.usgs.gov/faqs/what-are-band-designations-landsat-satellites?qt-news_science_products=0#qt-news_science_products. (Accessed: 15 December 2018).

[5] USGS, "USGS EROS Archive - Sentinel-2." USGS, 2019 https://www.usgs.gov/centers/eros/science/usgs-eros-archive-sentinel-2?qt-science_center_objects=0#qt-science_center_objects. (Accessed: 20 January 2019).

[6] Young, N. E., Anderson, R. S., Chignell, S. M., Vorster, A. G., Lawrence, R., and Evangelista, P. H., "A survival guide to landsat preprocessing," *Ecology* **98**(4), 920–932 (2017).

[7] Zhou, Y., Dong, J., Xiao, X., Xiao, T., Yang, Z., Zhao, G., Zou, Z., and Qin, Y., "Open surface water mapping algorithms: A comparison of water-related spectral indices and sensors," *Water* **9**(4), 256 (2017).

[8] Rouse Jr, J., Haas, R., Schell, J., and Deering, D., "Monitoring vegetation systems in the great plains with erts," (1974).

[9] Tucker, C. J., Holben, B. N., Elgin Jr, J. H., and McMurtrey III, J. E., "Remote sensing of total dry-matter accumulation in winter wheat," *Remote Sensing of Environment* **11**, 171–189 (1981).

[10] McFeeters, S. K., "The use of the normalized difference water index (ndwi) in the delineation of open water features," *International journal of remote sensing* **17**(7), 1425–1432 (1996).

[11] Xu, H., "Modification of normalised difference water index (ndwi) to enhance open water features in remotely sensed imagery," *International journal of remote sensing* **27**(14), 3025–3033 (2006).

[12] Feyisa, G. L., Meilby, H., Fensholt, R., and Proud, S. R., "Automated water extraction index: A new technique for surface water mapping using landsat imagery," *Remote Sensing of Environment* **140**, 23–35 (2014).

[13] Jiang, H., Feng, M., Zhu, Y., Lu, N., Huang, J., and Xiao, T., "An automated method for extracting rivers and lakes from landsat imagery," *Remote Sensing* **6**(6), 5067–5089 (2014).

[14] USGS, "USGS science for a changing world." USGS, 2019 https://earthexplorer.usgs.gov/. (Accessed: 10 July 2019).

[15] Chander, G., Markham, B. L., and Helder, D. L., "Summary of current radiometric calibration coefficients for landsat mss, tm, etm+, and eo-1 ali sensors," *Remote sensing of environment* **113**(5), 893–903 (2009).